Journal of Alloys and Compounds 688 (2016) 712–717

Contents lists available at ScienceDirect

Journal of Alloys and Compounds

journal homepage: http://www.elsevier.com/locate/jalcom

Highly sensitive gas sensor based on SnO_2 nanorings for detection of isopropanol

Shan-Hong Li [a], Zhong Chu [a], Fang-Fang Meng [a], Tao Luo [b], Xiao-Ye Hu [c, **], Su-Zhen Huang [d], Zhen Jin [b, *]

[a] Department of Electronic Information and Electrical Engineering, Hefei University, Hefei, Anhui 230601, PR China
[b] Research Center for Biomimetic Functional Materials and Sensing Devices, Institute of Intelligent Machines, Chinese Academy of Sciences, Hefei, Anhui 230031, PR China
[c] Key Laboratory of Materials Physics, and Anhui Key Laboratory of Nanomaterials and Nanostructures, Institute of Solid State Physics, Chinese Academy of Sciences, Hefei, Anhui 230031, PR China
[d] Institute of Plasma Physics, Chinese Academy of Sciences, Hefei, Anhui 230031, PR China

ARTICLE INFO

Article history:
Received 5 May 2016
Received in revised form
15 July 2016
Accepted 24 July 2016
Available online 26 July 2016

Keywords:
SnO_2
Nanorings
Isopropanol
Highly sensitivity

ABSTRACT

Isopropanol has been widely used as solvents and synthetic chemical intermediates in many field, but is very harmful volatile organic compound to human health. Therefore, monitoring of isopropanol is urgently needed. Here we report a facile hydrothermal method to SnO_2 nanorings, which can be used as gas sensing materials for isopropanol detection. Measurement results show that the SnO_2 nanorings have rapid response, and good repeatability, highly gas sensitivity to isopropanol, and achieving the detection of isopropanol with a low concentration of 1 ppm. Moreover, we also explained the formation mechanism of the SnO_2 nanorings, suggesting that bubbles-template-assisted growth mechanism dominates the formation of the SnO_2 nanorings. The synthesis approach to SnO_2 nanorings and the achievement of detection to isopropanol with a low concentration are of fundamental importance to synthesis of sensing materials and environmental sciences.

1. Introduction

Isopropanol is one of the most commonly volatile organic compounds (VOC), has been widely used as solvents and synthetic chemical intermediates in pesticides, printing, pharmaceutical, electronics, household chemical and many other fields [1,2]. However, isopropanol is very harmful to human health [3,4]. The isopropanol vapor with the concentration below 400 parts per million (ppm) results in irritation of the eyes, nose, mouth, and throat; and that with a higher concentration inhibits the central nervous system, or cause dizziness, severe vomiting, excessive sweating, vomiting, swelling and internal bleeding [5]. Therefore, effective monitoring of isopropanol is necessary for strengthening environmental regulations and treatments.

Semiconductor metal oxides gas sensors are the effective tools for detecting and monitoring various harmful gases and vapors, and have attracted great attention due to good performances, low cost, compact size and simple measuring electronics [6–8]. Generally, the performance of the semiconductor gas sensor is mainly dependent on the sensing materials [9]. It is well known that, among various sensing materials, tin oxide (SnO_2) is considered to be one of the most popular sensing materials because of its large excitation energy, excellent electronic and photonic properties [10,11]. Up to date, many efforts have been devoted to obtain high performance sensing material by tailoring the morphologies and structures of nanoscaled SnO_2 materials [12,13]. Furthermore, SnO_2 nanomaterials with various morphologies have been synthesized, such as nanowires [14], nanotubes [15], nanobelts [16] and microspheres [17,18]. But there are few reports on SnO_2 nanoring structure as gas sensor. In contrast, nanorings have porous structure, higher special surface area and slight agglomeration, being favorable to the adsorption and diffusion of target gas molecules, thus introducing better gas-sensing performance [19]. In consideration of the advantageous of SnO_2 nanorings to the gas-sensing performance, we here present a facile hydrothermal method to SnO_2 nanorings. As the sensing materials, the SnO_2 nanorings exhibit high response and short response and recovery times

* Corresponding author.
** Corresponding author.
E-mail addresses: hxy821982@issp.ac.cn (X.-Y. Hu), ftbjin@hotmail.com (Z. Jin).

http://dx.doi.org/10.1016/j.jallcom.2016.07.248
0925-8388/

towards isopropanol. Therefore, our synthesis approach to the SnO_2 nanorings gives a clue to the fabrication of the SnO_2 sensing materials with unique nanostructure and excellent sensing performance. To the best of our knowledge, there are only a few reports mentioned about the sensing properties of SnO_2 sensing materials to isopropanol, and the corresponding sensitivities are also not high [20]. Herein, the as-fabricated SnO_2 nanorings display high gas sensitivity to the isopropanol, achieving the detection of isopropanol with a low concentration of 1 ppm, thus being of fundamental importance to environmental sciences and human health.

2. Experimental

2.1. Synthesis of the SnO_2 nanorings

All reagents are commercially available from Sinopharm Chemical Reagent Co., Ltd. (China) with analytical grade and without further purification.

For the synthesis of SnO_2 nanorings, 0.3 g of $SnCl_4 \cdot H_2O$ and 0.9 g of urea are firstly dissolved into 40 mL of deionized water with vigorously stirring for 30 min. The transparent solution is obtained, and then transferred into a 50 mL Teflon-lined stainless autoclave, sealed and heated at 150 °C for 300 min, finally cooled to room temperature naturally. The resultant precipitate is then centrifuged, washed, and dried at 60 °C. Finally, the SnO_2 powder is obtained after annealing the precursor at 500 °C for 2 h in air atmosphere.

2.2. Characterization

The morphologies of the as-prepared products are characterized by field-emission scanning electron microscopy (FE-SEM, FEI Sirion-200), high resolution transmission electron microscopy (HRTEM, JEOL JEM-2011). The crystal structure of the as-prepared samples is determined by X-ray diffraction (XRD, Philips X'pert PRO) with Cu K radiation. Energy dispersive spectroscopy (EDS) is measured by Oxford INCA X-Max 50.

2.3. Fabrication of the gas sensor and the gas sensing measurement system

The structure of the gas sensor is schematically shown in Fig. 1a. A pair of gold electrodes is firstly fabricated onto a ceramic tube by thick film technology. And then two pairs of gold wires are connected to them. A piece of nichrome wire with the resistance of 30 Ω is placed in the interior of the ceramic tube as heating wire. To fabricate a gas sensor, the as-prepared samples of the SnO_2 nanorings or commercial SnO_2 powders are directly coated on the surface of the ceramic tube and dried in infrared drying oven, and then sintered in muffle furnace at 350 °C for 2 h in air.

Typically, as shown in Fig. 1b, a gas sensing measurement is performed in a closed test chamber with a volume of about 1000 mL equipped with appropriate an inlet and an outlet for gas flow. A Keithley 6487 Source/Measure Unit (SMU) is used to measure the film thickness. The as-deposited films are applied for the measurement of gas sensing properties. The gas sensing properties are evaluated at various operation temperatures from 100 to 400 °C by measuring the changes of resistance of the sensor in air. The target gas is prepared by drawing out the headspace vapor into a microsyringe at room temperature. And the low concentrations of samples are prepared by diluting the vapors in a vessel before injecting them into the test chamber. The response of the sensor is defined as:

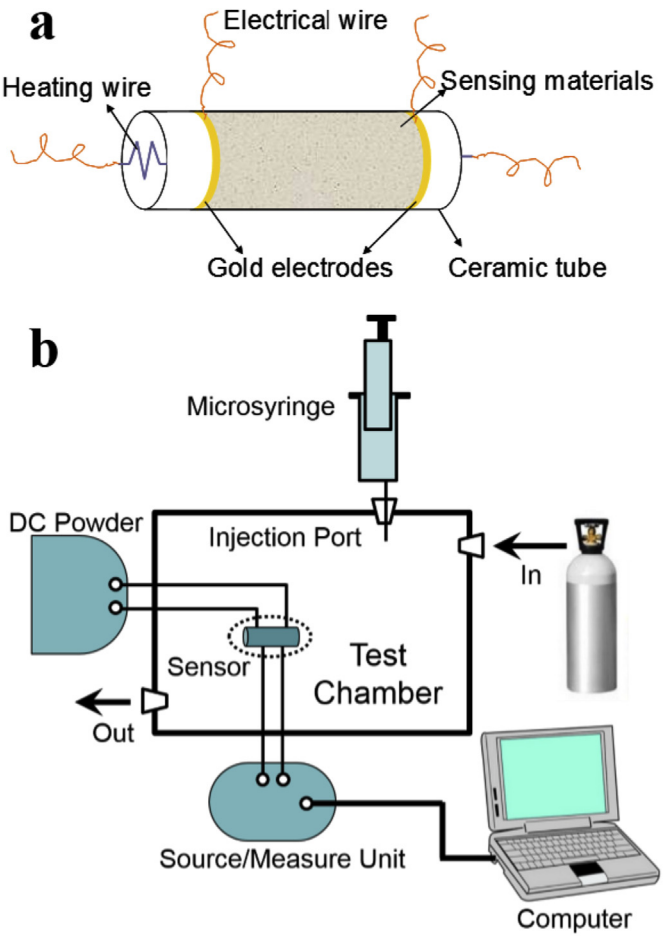

Fig. 1. The schematic diagram of the gas sensor (a) and the experimental setup (b).

$$\text{Response} = \frac{I_g - I_a}{I_a} \times 100\% \quad (1)$$

Here, I_a and I_g are the electric currents of the sensor in air and target gas, respectively.

3. Results and discussion

Fig. 2 presents the XRD pattern of the obtained products,

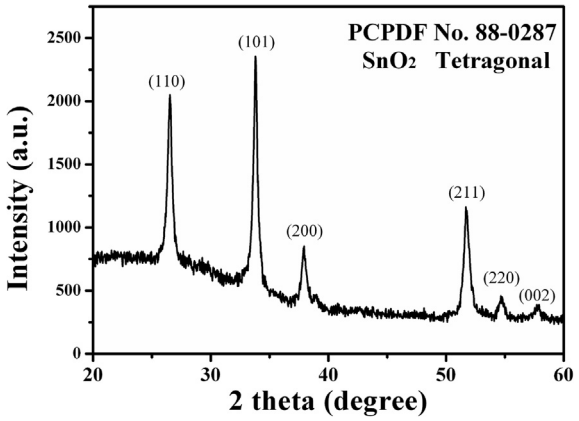

Fig. 2. The XRD pattern of the SnO_2 nanorings.

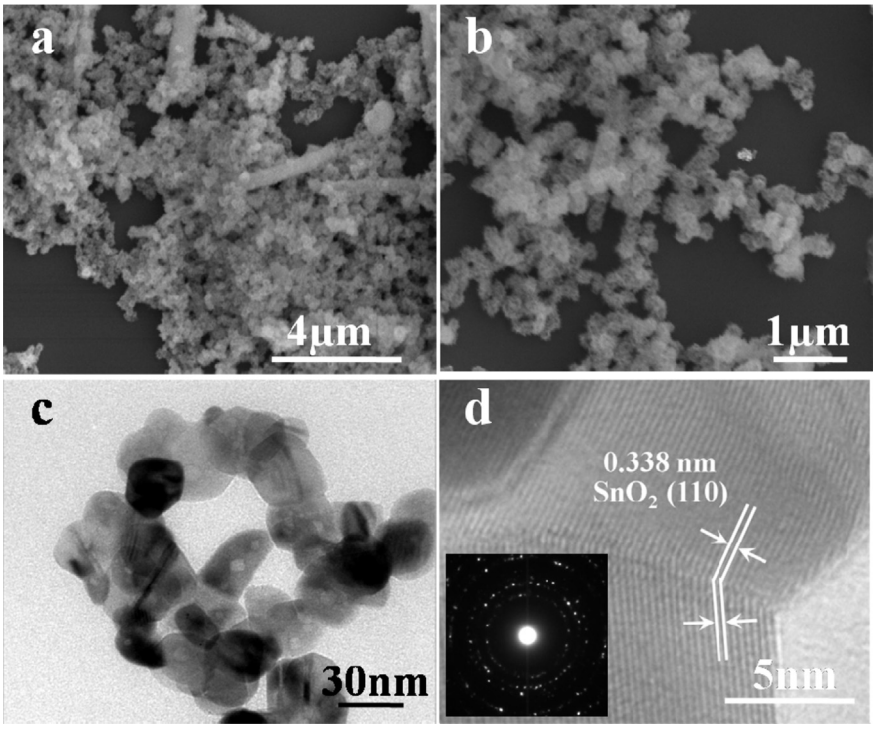

Fig. 3. (a) Low and (b) high magnification SEM images of the SnO_2 nanorings, (c) TEM image of the SnO_2 nanorings, (d) the lattice-resolved HRTEM image inserted with corresponding SAED pattern of the SnO2 nanorings.

revealing that all of the diffraction peaks can be indexed to tetragonal SnO_2 (PCPDF No. 88–0287). That is to say, the as-obtained products are tetragonal SnO_2, which is the most stable and most common phase. The results of morphology characterization show that the SnO_2 powders are loose structures (Fig 3a), consists of a large amount of self-assembled nanoparticles (Fig 3b). TEM images manifest that the nanoparticles self-assemble into ring-like structures with about 60–100 nm in the diameter (Fig. 3c and d). The SAED pattern of the nanoparticle (inset of Fig. 3d) presents series of concentric rings with different diameters, corresponding to the nature lattice planes of tetragonal SnO_2. HRTEM image shows the fringe spacing are 0.338 nm, which match well with the (110) lattice space of the tetragonal SnO_2. Meanwhile, the HRTEM image also indicates that, in different nanoparticles, the lattice fringes are oriented attached, forming a continuous crystal lattice.

For the formation mechanism of the SnO_2 nanorings, we suggest a bubbles-template-assisted growth mechanism. The formation process of the SnO_2 nanoring can be intuitively and schematically displayed as Fig. 4. During the hydrothermal treatment, urea is firstly decomposed to form large amount of hydroxyl ions and CO_2 bubbles. At the moment, the SnO_2 nanoparticles (or sub-nm seeds) with smaller size are formed, dispersing in the whole solution (Fig. 4a). The CO_2 bubbles can be considered as a template (Fig. 4b), resulting in the adsorption of SnO_2 seeds on the surface of the CO_2 bubbles, and then growing along the surface of the CO_2 bubbles.

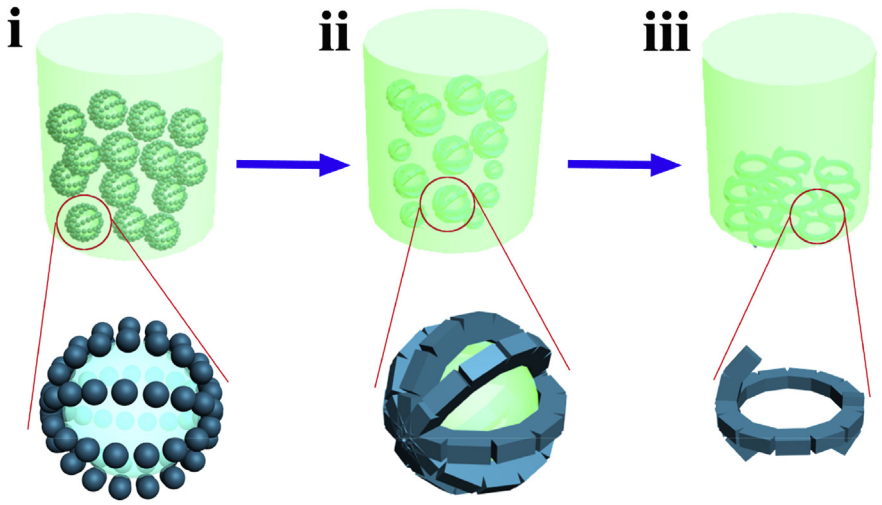

Fig. 4. The schematical formation process of the SnO_2 nanorings.

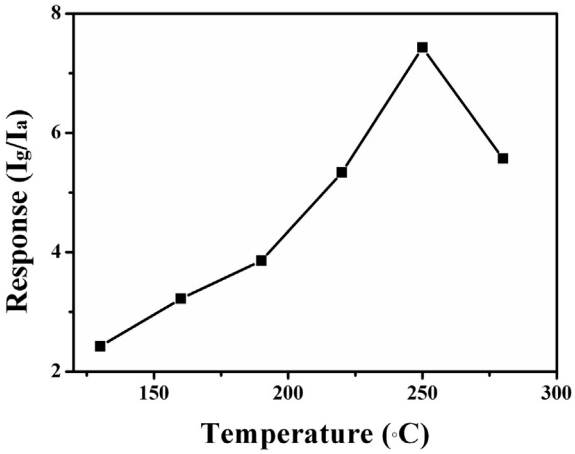

Fig. 5. Responses of the SnO_2 nanorings to 100 ppm of isopropanol at different operating temperatures at different operating temperatures.

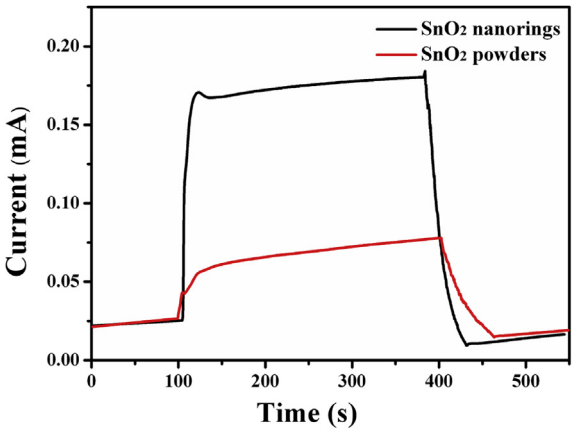

Fig. 7. Comparison of the SnO_2 nanorings sensor and commercial SnO_2 powder sensor to 100 ppm of isopropanol vapor.

However, the CO_2 bubbles are not stable, easily escape and burst resulting from the fluctuation of the solution, leading to the SnO_2 nanoparticles to assemble into incomplete spheres or rings, as shown Fig. 4c. In addition, it should be noted that the SnO_2 nanoparticles assemble on the surface of the CO_2 bubbles according to the oriented attachment mechanism, bring about the continuous crystal lattice between interfacing nanoparticles, as confirmed by the HRTEM image (Fig. 3c). The continuous crystal lattice is benefit for electron transport during the whole nanorings.

Next, the as-synthesized SnO_2 nanorings are used as sensing materials to detect the isopropanol via the gas sensitivity test, which can not only estimate the sensing performance of the SnO_2 nanorings, but also achieve the practical application for the sensitive detection of isopropanol (high toxicity and long-term existing in the environment). Prior to the gas sensitivity test, the operating temperature that is very important for the sensing performance of metal oxide gas sensors, must be determined. Therefore, we systematically investigated that the responses of the SnO_2 nanoring to 100 ppm of isopropanol at different operating temperatures (Fig. 5). Obviously, the responses firstly increase and then present a turning point at 250 °C with increasing operating temperature, indicating the optimal operating temperature is 250 °C. According to Wolkenstein's model for semiconductors [21], the surface reactions of the target gases are usually highly dependent on the activity of the adsorbed oxygen species. Either molecular (O^{2-}) or atomic (O^{-}, O^{2-}) oxygen species are present on the surface at different temperature. Generally, the molecular form works mostly below 150 °C, while the atomic species play a dominant role at higher temperature [22]. The optimal operating temperature of 250 °C suggests that the atomic species dominates the metal oxide gas sensor. Thus, we determine that the gas sensitivity tests are carried out at 250 °C.

The sensitivity of the SnO_2 nanorings to isopropanol is shown in Fig. 6a. With the increasing of the isopropanol gas concentration from 1 to 500 ppm, the current increases, and rapidly drop as the isopropanol gas is removed from the testing atmosphere. Fig. 6b displays the plot of the current intensity as a function of the isopropanol of different concentration, revealing a linear range from 1 to 500 ppm. The least-squares fitting was $y = 2.46 + 0.069 \cdot x$ with a regression coefficient (R^2) of 99.7%. The results reveal that the SnO_2 nanorings have good response for isopropanol. Compared with the commercial SnO_2 powders (Fig. 7), the response and recovery time of SnO_2 nanorings to 100 ppm of isopropanol are 6.8 and 38.6 s, respectively, which is better than that (about 21.5 and 58.3 s) of the commercial SnO_2 powders. In addition, the response of commercial SnO_2 powders is 2.76, but that of the SnO_2 nanorings is 7.27. Table 1 shows the parameters of reported isopropanol sensors based on different metal oxide nanostructures. As we can see, the current lowest detection concentration only reaches the level of 100 ppm. However, the lowest detection concentration of the SnO_2 nanorings reaches 1 ppm, which is much lower than other reports. Thus, the SnO_2 nanorings possessed higher response and shorter response

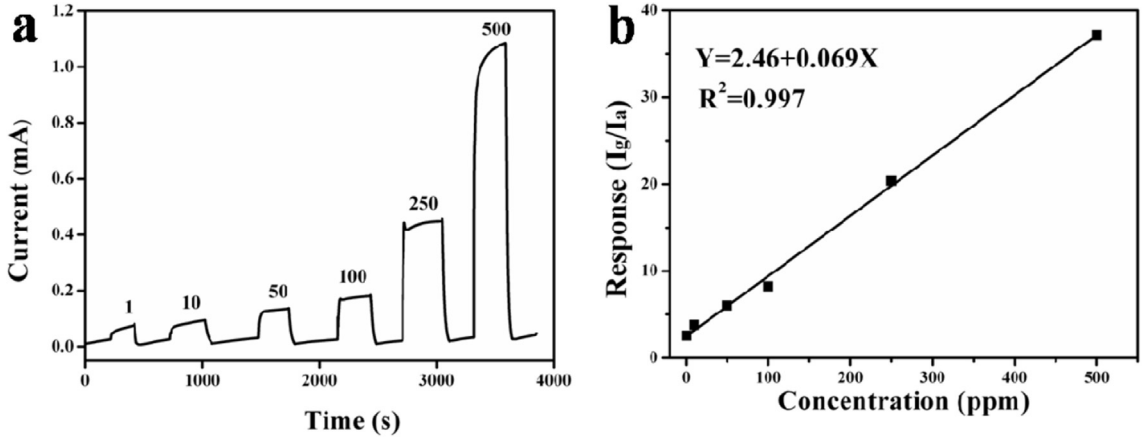

Fig. 6. (a) Real-time responses of the SnO_2 nanorings to isopropanol at 300 °C and (b) the corresponding plots of the response vs concentration.

Table 1
Isopropanol sensors based on metal oxide nanostructures.

Sensing materials	Lowest detection concentration	Operating temperature	Ref.
SnO_2 nanorods	100 ppm	450 °C	[20]
ZnO–CdO composites	100 ppm	248 °C	[23]
TeO_2 nanowires	100 ppm	50 °C	[24]
PbO-doped SnO_2	500 ppm	250 °C	[25]
SnO_2 nanorings	1 ppm	250 °C	Present work

and recovery times, displaying excellent gas sensitivity.

Moreover, the SnO_2 nanorings also exhibit rather good stability and repeatability. Fig. 8 shows the response of the SnO_2 nanorings to 100 ppm of isopropanol after 10 cycles of gas on and off at 250 °C, manifesting that the maximum deviation is an acceptable range. Based on the high sensitivity and good repeatability, the SnO_2 nanoring might become a good sensing material for promising industrial applications. For practical application, it is also necessary that gas sensor devices possess high selectivity. Previous reports indicate that SnO_2 nanostructure based sensors have responses to many gases, including ethanol, benzene, toluene, etc. However, in our case, the response of the SnO_2 nanorings to 100 ppm of isopropanol is much higher than that to 100 ppm of other gases, as shown Fig. 9. This result speaks volumes for the excellent selectivity of SnO_2 nanorings to isopropanol.

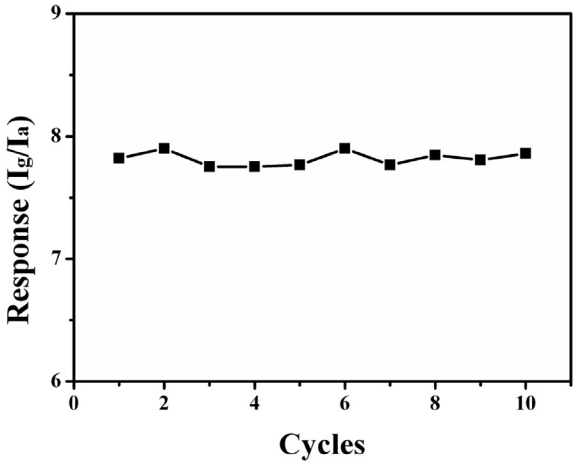

Fig. 8. Stability of the SnO_2 nanorings to 100 ppm of isopropanol at 250 °C.

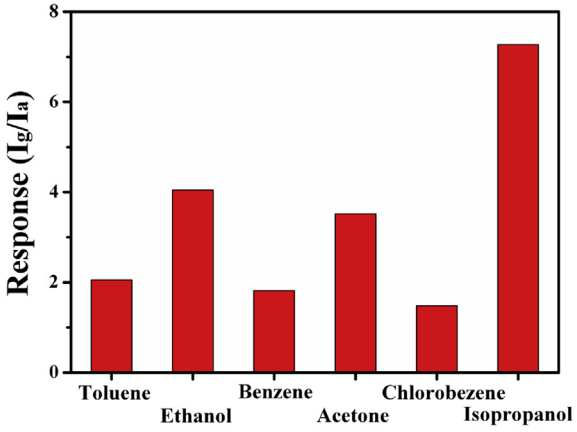

Fig. 9. Comparison of the responses of the SnO_2 nanorings to 100 ppm of different VOCs.

4. Conclusion

In conclusion, we have synthesized the SnO_2 nanorings assembled by nanoparticles through a facile hydrothermal method. The SnO_2 nanorings used as gas sensing materials displays excellent the high sensitivity, achieving the detection of isopropanol with a low concentration of 1 ppm. Moreover, compared with commercial SnO_2 powders, the SnO_2 nanorings have rapid response, good repeatability and high sensitivity to isopropanol. Meanwhile, the SnO_2 nanorings possess high selectivity to isopropanol. Therefore, we suggest that the synthesis approach to SnO_2 nanorings and the achievement of detection to isopropanol with a low concentration are of fundamental importance to environmental sciences and human health.

Acknowledgements

We appreciate the financial support of the Natural Science Research Project of Anhui Educational Committee (No. KJ2016A598, No. KJ2016A600), the National Natural Science Foundation of China (No. U1432140), Key Project of Scientific Research Foundation of Hefei University (No. 10KY02ZD), and Scientific Research Foundation for Talents of Hefei University (No. 14RC11).

References

[1] H.G. Premakshi, A.M. Sajjan, M.Y. Kariduraganavar, Development of pervaporation membranes using chitosan and titanium glycine-N,N-dimethylphosphonate for dehydration of isopropanol, J. Mater Chem. A 3 (2015) 3952–3961.
[2] K. Larmier, C. Chizallet, N. Cadran, S. Maury, J. Abboud, A.F. Lamic-Humblot, E. Marceau, H. Lauron-Pernot, Mechanistic investigation of isopropanol conversion on alumina catalysts: location of active sites for alkene/ether production, Acs Catal. 5 (2015) 4423–4437.
[3] Y. Shao, H.H. Chen, Y.B. Li, X.O. Ma, Fabrication of novel porous carbon membrane/sintered metal fibers composite for isopropanol adsorption, Chem. Eng. J. 276 (2015) 51–58.
[4] P. Cabeza, B. Al-Duri, M.D. Bermejo, M.J. Cocero, Co-oxidation of ammonia and isopropanol in supercritical water in a tubular reactor, Chem. Eng. Res. Des. 92 (2014) 2568–2574.
[5] Y.L. Wu, Q.P. Luan, S.J. Chang, Z.Y. Jiao, W.Y. Weng, Y.H. Lin, C.L. Hsu, Highly sensitive beta-Ga_2O_3 nanowire nanowires isopropyl alcohol sensor, Ieee Sens. J. 14 (2014) 401–405.
[6] Z.H. Jing, J.H. Zhan, Fabrication and gas-sensing properties of porous ZnO nanoplates, Adv. Mater 20 (2008) 4547–4551.
[7] F.L. Meng, N.N. Hou, Z. Jin, B. Sun, Z. Guo, L.T. Kong, X.H. Xiao, H. Wu, M.Q. Li, J.H. Liu, Ag-decorated ultra-thin porous single-crystalline ZnO nanosheets prepared by sunlight induced solvent reduction and their highly sensitive detection of ethanol, Sens. Actuat B-Chem 209 (2015) 975–982.
[8] E. Brunet, T. Maier, G.C. Mutinati, S. Steinhauer, A. Kock, C. Gspan, W. Grogger, Comparison of the gas sensing performance of SnO_2 thin film and SnO_2 nanowire sensors, Sens. Actuat B-Chem 165 (2012) 110–118.
[9] F.L. Meng, S. Ge, Y. Jia, B. Sun, Y.F. Sun, C. Wang, H. Wu, Z. Jin, M.Q. Li, Interlaced nanoflake-assembled flower-like hierarchical ZnO microspheres prepared by bisolvents and their sensing properties to ethanol, J. Alloy Compd. 632 (2015) 645–650.
[10] B.W. Zhang, W.Y. Fu, H.Y. Li, X.L. Fu, Y. Wang, H. Bala, X.D. Wang, G. Sun, J.L. Cao, Z.Y. Zhang, Synthesis and characterization of hierarchical porous SnO_2 for enhancing ethanol sensing properties, Appl. Surf. Sci. 363 (2016) 560–565.
[11] F. Gao, G.H. Qin, Y.H. Li, Q.P. Jiang, L. Luo, K. Zhao, Y.J. Liu, H.Y. Zhao, One-pot synthesis of La-doped SnO_2 layered nanoarrays with an enhanced gas-sensing performance toward acetone, Rsc Adv. 6 (2016) 10298–10310.
[12] C.L. Zhang, J. Wang, R.J. Hu, Q. Qiao, X.G. Li, Synthesis and gas sensing properties of porous hierarchical SnO_2 by grapefruit exocarp biotemplate, Sens.

Actuat B-Chem 222 (2016) 1134–1143.
[13] H.B. Ren, W. Zhao, L.Y. Wang, S.O. Ryu, C.P. Gu, Preparation of porous flower-like SnO_2 micro/nano structures and their enhanced gas sensing property, J. Alloy Compd. 653 (2015) 611–618.
[14] Y. Sun, J. Liu, D. Blom, G. Koley, Z.Y. Duan, G.F. Wang, X.D. Li, Atomic-scale imaging correlation on the deformation and sensing mechanisms of SnO_2 nanowires, Appl. Phys. Lett. 105 (2014).
[15] P. Wu, X.L. Xu, Q.Y. Zhu, X.S. Zhu, Y.W. Tang, Y.M. Zhou, T.H. Lu, Self-assembled graphene-wrapped SnO_2 nanotubes nanohybrid as a high-performance anode material for lithium-ion batteries, J. Alloy Compd. 626 (2015) 234–238.
[16] Z. Guo, X. Chen, J.H. Liu, X.J. Huang, Transport phenomena and conduction mechanism of individual cross-junction SnO_2 nanobelts, Small 9 (2013) 2678–2683.
[17] X.B. Wang, Y.Y. Wang, F. Tian, H.J. Liang, K. Wang, X.H. Zhao, Z.S. Lu, K. Jiang, L. Yang, X.D. Lou, From the surface reaction control to gas-diffusion control: the synthesis of hierarchical porous SnO_2 microspheres and their gas-sensing mechanism, J. Phys. Chem. C 119 (2015) 15963–15976.
[18] Y.F. Wang, X.F. Li, D.J. Li, Y.W. Sun, X.X. Zhang, Controllable synthesis of hierarchical SnO_2 microspheres for dye-sensitized solar cells, J. Power Sources 280 (2015) 476–482.
[19] C. Li, Y. Lin, F. Li, L.H. Zhu, F.X. Meng, D.M. Sun, J.R. Zhou, S.P. Ruan, Synthesis and highly enhanced acetylene sensing properties of Au nanoparticle-decorated hexagonal ZnO nanorings, Rsc Adv. 5 (2015) 87132–87138.
[20] D. Hu, B.Q. Han, R. Han, S.J. Deng, Y. Wang, Q. Li, Y.D. Wang, SnO_2 nanorods based sensing material as an isopropanol vapor sensor, New J. Chem. 38 (2014) 2443–2450.
[21] H. Haick, M. Ambrico, T. Ligonzo, R.T. Tung, D. Cahen, Controlling semiconductor/metal junction barriers by incomplete, nonideal molecular monolayers, J. Am. Chem. Soc. 128 (2006) 6854–6869.
[22] N. Barsan, U. Weimar, Conduction model of metal oxide gas sensors, J. Electroceram 7 (2001) 143–167.
[23] X.Y. Cai, D. Hu, S.J. Deng, B.Q. Han, Y. Wang, J.M. Wu, Y.D. Wang, Isopropanol sensing properties of coral-like ZnO-CdO composites by flash preparation via self-sustained decomposition of metalorganic complexes, Sens. Actuat B-Chem 198 (2014) 402–410.
[24] Y.B. Shen, A.F. Fan, D.Z. Wei, S.L. Gao, W.G. Liu, C. Han, B.Y. Cui, A low-temperature n-propanol gas sensor based on TeO_2 nanowires as the sensing layer, Rsc Adv. 5 (2015) 29126–29130.
[25] J.K. Srivastava, P. Pandey, V.N. Mishra, R. Dwivedi, Structural and micro structural studies of PbO-doped SnO_2 sensor for detection of methanol, propanol and acetone, J. Nat. Gas. Chem. 20 (2011) 179–183.